Published in: *Colloids & Surfaces A* **128** (1997) 155–175

STABILITY OF EMULSIONS UNDER EQUILIBRIUM AND DYNAMIC CONDITIONS

Ivan B. Ivanov[1] and Peter A. Kralchevsky

Laboratory of Thermodynamics and Physico-chemical Hydrodynamics, University of Sofia, Faculty of Chemistry, Sofia 1126, Bulgaria

ABSTRACT

In the present article we analyze the influence of various factors, both thermodynamic and hydrodynamic, on the stability of emulsion systems. The effect of the droplet size on the droplet life-time in an emulsion cream is quantified. The comparative importance of kinetic factors such as surface and bulk diffusion fluxes, or viscous and elastic surface stresses, is investigated. The fact that the emulsion films drain much slower when the surfactant is dissolved in the continuous phase (rather than in the disperse phase) provides a new understanding of the Bancroft rule and the process of chemical demulsification. New thermodynamic aspects of emulsion stability are also discussed. One of them is the relatively high surface electric potential of pure oil-water interfaces and adsorption monolayers of nonionic surfactants. Another aspect is the role of non-DLVO surface forces, such as the hydration repulsion, oscillatory structural and depletion forces due to the presence of surfactant micelles. A criterion of emulsion stability is formulated synthesizing the effects of the major factors. Finally we consider the importance of the kinetic phenomena in emulsions formed from non-preequilibrated phases.

[1] Author to whom correspondence should be addressed; e-mail: ii@lcpe.uni-sofia.bg

1. Introduction

The collision of two emulsion droplets may be accompanied by deformation (flattening in the zone of contact) depending on the energy of interaction between the droplets (the conditions for flattening are investigated in Refs. [1-3]). In general, the gap between two non-deformed particles (Figure 1) can be considered as a liquid film of *uneven* thickness. In the latter case the calculation of the particle-particle interaction energy can be reduced to the simpler calculation of the interaction across a plane-parallel film by using the Derjaguin approximation [4,5]. In addition, comparatively large thin liquid films exist in the concentrated emulsions of foam-like structure. One can expect that the stability of the emulsions is to a great extent determined by the properties of the thin liquid films (including those of uneven thickness) under equilibrium and dynamic conditions.

There are three scenarios for the behavior of two colliding droplets in an emulsion depending on the properties of the films (Fig. 1). (i) When the film formed upon particle collision is stable, flocks of attached particles can appear. (ii) When the attractive interaction across the film is predominant, the film is unstable and ruptures; this leads to a coalescence of the drops in emulsions or of the bubbles in foams. (iii) If the repulsive forces are predominant, the two colliding particles will rebound and the emulsion will be stable. In some cases, by varying the electrolyte concentration or pH, it is possible to increase the repulsion between the particles in a flocculated dispersion and to cause the inverse process of peptisation [6].

In addition to the surface forces of intermolecular origin (the disjoining pressure), two colliding particles in a liquid medium experience also *hydrodynamic* interactions due to the viscous friction, which can be rather long range (operative even at distances above 100 nm). The hydrodynamic interaction among particles depends on both the type of fluid motion and the type of interfaces. Usually the effect of the hydrodynamic interaction is expressed as a relation between the particle velocity and the driving force. For example, the velocity of approach of two parallel solid discs, V_{Re}, under the action of applied force, F_z, is given by the Reynolds formula [7,8]

$$V_{\mathrm{Re}} = \frac{2F_z h^3}{3\pi\eta R^4} = \frac{2\left[P_c - \Pi(h)\right]h^3}{3\eta R^2} \tag{1.1}$$

where h is the distance between the discs (the film thickness), R is the disc (film) radius, η is the viscosity of the film phase; in the case of film between two colliding droplets (bubbles) the driving force can be expressed in the form $F_z = \left[P_c - \Pi(h)\right]R^2$, where Π is the disjoining pressure of the film, and $P_c = 2\sigma / R_d$ is the capillary pressure of the droplet with σ and R_d being the interfacial tension and the droplet radius. Eqn (1.1) is currently used [9] to describe the velocity of thinning of foam or emulsion films of tangentially immobile surfaces (immobilized due to the presence of dense surfactant adsorption monolayers). In the case of two axisymmetric

particles moving along the z-axis towards each other with velocity $V = -dh/dt$ the film life-time can be estimated by means of the expression [9]

$$\tau = \int_{h_c}^{\infty} \frac{dh}{V} = \frac{3\eta R^2}{2} \int_{h_c}^{\infty} \frac{dh}{[P_c - \Pi(h)]h^3} \tag{1.2}$$

where at the last step we have substituted $V = V_{\mathrm{Re}}$ from Eqn (1.1), and h_c is the critical thickness of film rupture. On the other hand, the film can reach a thermodynamic equilibrium state corresponding to film thickness h_e, which satisfies the relation

$$\Pi(h_e) = P_c \tag{1.3}$$

In the case when $h_e < h_c$ the thinning film will rupture before reaching an equilibrium state, i.e. the film will have a finite life-time τ determined by Eqn (1.2). In the case when $h_e > h_c$ the thinning film may eventually reach an equilibrium state; for this case Eqn (1.2) predicts an infinite life-time.

In the more general case of two droplets of different radii, R_1 and R_2, film radius R and uniform film thickness h (see Fig. 2) the following expression can be derived [2]:

$$F_z = \frac{3}{2}\pi\eta V \frac{R_*^2}{h}\left(1 + \frac{R^2}{hR_*} + \frac{R^4}{h^2 R_*^2}\right), \qquad R_* \equiv 2R_1R_2/(R_1+R_2). \tag{1.4}$$

This geometrical configuration is proved to be very close to the real one in the presence of electrostatic disjoining pressure [10].

Setting R=0 in Eqn (1.4) one can derive a generalized version of the *Taylor formula* [11] for the velocity of approach of two non-deformed spherical droplets under the action of an external force F_z:

$$V_{\mathrm{Ta}} = \frac{2hF_z}{3\pi\eta R_*^2} \tag{1.5}$$

When a non deformed sphere of radius R_c approaches a flat solid surface one may use the Taylor formula with R_*=2R_c when the gap between the two surfaces is small compared to R.

2. Effect of the droplet size on the life-time of emulsion films

The emulsion stability correlates well with the lifetime of separate thin emulsion films or of drops coalescing with their homophase, as indicated by the experiment [12-14]. To simplify the treatment we will consider here the life-time of a single drop pressed against its homophase under the action of gravity. To define the *life-time* (or drainage time) τ we assume that in the

initial and final moments the film has some known thicknesses h_{in} and h_f. Then one combines Eqns (1.2) and (1.4) to derive [15]:

$$\tau = \int_{h_f}^{h_{in}} \frac{dh}{V_z} = \frac{3\pi\eta R_*^2}{2F_z}\left[\ln\left(\frac{h_{in}}{h_f}\right) + \frac{R^2}{h_f R_*}\left(1-\frac{h_f}{h_{in}}\right) + \frac{R^4}{2h_f^2 R_*^2}\left(1-\frac{h_f^2}{h_{in}^2}\right)\right] \tag{2.1}$$

The final thickness, h_f, may coincide with the critical thickness of film rupture. The expression (2.1) is derived for tangentially immobile interfaces at fixed driving force F_z (no disjoining pressure).

In the case of gravity driven *coalescence of a droplet with its homophase*, the driving force (the buoyancy force) and the mean drop radius are

$$F_z = \frac{4}{3}\pi R_d^3 g\Delta\rho \quad , \quad R_* = 2R_d \tag{2.2}$$

where g is the gravity acceleration, $\Delta\rho$ is the density difference and R_d is the droplet radius. The film radius can be estimated from the balance of the driving and capillary force [9]:

$$R^2 = \frac{F_z R_d}{2\pi\sigma} \tag{2.3}$$

Combining Eqns (2.1)-(2.3) one can calculate the dependence of the life (drainage) time τ vs. the droplet radius R_d. Numerical results are plotted in Fig. 3 for parameters values typical for emulsion systems: $\Delta\rho$=0.2 g/cm^3, η=1 cP, h_f = 5 nm, and $h_{in} = R_d/10$. The various curves in Fig. 3 correspond to different values of the surface tension σ, shown in the figure. The left branches of the curves correspond to the Taylor regime (non-deformed droplets), whereas the right branches correspond to the Reynolds regime (formation of film between the droplets). In particular, the data of Dickinson *et al.* [16] correspond to the left branch (Fig. 3); in addition, there is also data [9] complying with the right branch. The presence of a deep minimum on the τ vs. R_d curves was first pointed out in Ref. [17].

The asymptotics for small R_d (Taylor regime, non-deformed droplets) can be deduced by setting formally R=0 in Eqns (2.1) and (2.2):

$$\tau_{Ta} = \frac{6\pi\eta R_d^2}{F_z}\ln\left(\frac{h_{in}}{h_f}\right) = \frac{9\eta}{2gR_d\Delta\rho}\ln\left(\frac{h_{in}}{h_f}\right) \tag{2.4}$$

One sees that τ_{Ta} depends logarithmically on the ratio of the initial and final thickness. Moreover, in the Taylor regime the life-time τ decreases with the increase of the driving force, F_z, and the drop radius, R_d (see the lower curve in Fig. 3) in agreement with the experiment [16].

In the case of larger R_d (deformed drops, $R \neq 0$, *Reynolds regime* - the right branches of the curves in Fig.3) the life-time τ increases with the increase of the drop radius, R_d. This is exactly the opposite trend as compared with the result for Taylor regime, cf. Eqn (2.4). The result can be rationalized in view of the Reynolds equation, Eqn (1.1). In the numerator of this equation $F_z \propto R_d^3$, cf. Eqn (2.2), whereas in the denominator $R^4 \propto R_d^8$, cf. Eqn (2.3); as a result, the drainage rate become proportional to R_d^{-5}, i.e. V decreases as the droplet radius increases.

3. Stages of film thinning; thermodynamic and kinetic stability

An useful tool for studying the life-times of emulsion films, as well as the equilibrium film thicknesses is the Scheludko cell [18], see Fig. 4. The radius of the films in such a cell is typically $R \approx 1$ mm. Experimental cell allowing measurements at higher capillary pressures was constructed by Mysels, who used a hole in a porous plate [19]. Another cell allowing measurements with small films (R between 5 and 50 μm) was constructed by Velev et al. [20]. The stages of thinning of the investigated films are described and discussed below.

The experimental studies show that the thinning of a liquid film typically exhibits the following consecutive stages (Fig. 5):

(a) At large separations h between their caps, two drops (bubbles) will be only slightly deformed by the viscous friction. The shape of the gap between two drops for different characteristic times is calculated numerically by Yiantsios et al. [21,22]. Experimental investigation of these effects for symmetric and asymmetric drainage of foam films has been carried out by Joye *et al.* [23,24].

(b) At a smaller distance h_i the viscous forces become large enough to overcome the capillary forces and to deform the caps to a bell-shaped formation called *dimple* [25]. There is a number of theoretical studies describing the development of a dimple at the initial stage of film thinning [21,22,26-29]. The inversion thickness, h_i, can be calculated from the simple relation [30,31]

$$h_i = \frac{F_z\left(\sigma_1 + \sigma_2\right)}{4\pi\sigma_1\sigma_2} \tag{3.1}$$

where σ_1 and σ_2 are the interfacial tensions of the two phase boundaries; as usual, F_z is the force experienced by the approaching particles. Danov *et al*. [2] have derived expression for h_i for the case of *Brownian* flocculation of identical small droplets.

(c) The dimple is *usually* (for drops smaller than 1 mm) pushed away or gradually disappears and a planar film forms. Sometimes such films (usually the very small ones in the presence of enough surfactant) thin down gradually to some equilibrium thickness. The resulting plane-parallel film thins at almost constant radius R. When the electrostatic repulsion is strong, a thicker primary film forms (see point 1 in Fig. 6). From the viewpoint of the conventional DLVO theory

this film must be metastable. Indeed, the experiments [32] with microscopic foam films, stabilized with sodium octyl sulfate or sodium dodecyl sulfate in the presence of different amount of electrolyte show that black spot may suddenly form and a transition to secondary (Newton black) film may occur (see point 2 in Fig. 6).

(d) The surfaces of the primary film are always corrugated (due to external or hydrodynamic perturbations or to thermal fluctuations). As the film thins, the *attractive* interactions grow stronger and in some cases at a *critical thickness* h_c the film surfaces lose their stability, bend and at a given place touch each other. If the repulsion is weak, at that moment the film ruptures and coalescence takes place. The theory of film stability is developed by de Vries [33], Vrij [34], Ivanov *et al*. [35], Maldarelli et al. [36,37]; for a recent review see Refs. [15,31].

(e) If there is enough surfactant to create *strong repulsion* the two touching surfaces form a thinner (black) spot, called Newton Black Film (NBF). Such spots, which are nuclei of equilibrium thinner films, expand and/or coalesce with other spots, until the whole film is transformed into a NBF. The typical thickness of the plane-parallel films at stage "c" (Fig. 5 c) is about 200 nm , while the characteristic thickness h_2 of the Newton black film (Fig 5 e,f) is about 5-10 nm.

(f) The NBF can exist in equilibrium with the meniscus (the Plateau border) only at larger contact angle θ. This causes expansion of the whole film until the final equilibrium radius is reached. For more details about this last stage of film thinning see part IV.C of Ref. 31.

The existence of *thermodynamic* stable state(s) of a thin liquid film is determined by the roots of Eqn (1.3), i.e. by the intersection points of the line $\Pi = P_c$ =const with the Π(h)-isotherm, Fig.6. For lower values of the capillary pressure ($P_c = P_c'$) there can be two *stable* equilibrium states, whereas for higher values of the capillary pressure ($P_c = P_c''$) there is only one *stable* equilibrium state, Fig. 6.

It should be noted that the mere fact of existence of *thermodynamic* stable state(s) of a thin liquid film does not guarantee that the film can reach "safely" this state. Indeed, the film thinning is accompanied with convective and diffusion fluxes, vortices and instabilities, non-uniform surfactant adsorption, etc., cf. Fig.5. Each of these factors or their combination may lead to the rupture of the film before reaching the equilibrium state. Therefore, the concept for *kinetic stability* of thin liquid films is also used to denote the resistance of the film against rupture during the thinning. The major factor providing *kinetic* stability of emulsions is the presence of surfactant adsorption monolayers at the droplet surfaces.

4. Role of surfactant adsorption and solubility for the kinetic stability

4.1. Basic equations

The gap between two colliding droplets (bubbles) is depicted in Fig. 7. The convective flux of the liquid expelled from the gap carries along the adsorbed surfactant molecules from the center to the periphery of the two film surfaces (Fig. 7). The decreased surfactant adsorption in the central zone triggers (i) *bulk* diffusion flux of surfactant (**j** in Fig. 7) and (ii) *surface* diffusion flux of surfactant ($\mathbf{j}_s$ in Fig.7); both of them tend to suppress the deviation of the surfactant adsorption from its equilibrium value.

The equations of hydrodynamics and diffusion, describing the above processes can be simplified by using the axial symmetry of the system, the lubrication approximation ($h/R << 1$) and assuming small deviations from equilibrium of the surfactant concentration ($\delta c << c_o$) and adsorption ($\delta\Gamma << \Gamma_0$) [9,31,38,39].

The above simplifications allow one to write the equations of the *surfactant mass balance* in the form [9]

$$\frac{\partial^2 c}{\partial r^2} + \frac{\partial^2 c}{\partial z^2} = 0 \qquad \text{(bulk diffusion)} \qquad (4.1)$$

$$\Gamma_0 \frac{\partial v_r}{\partial r} - D_S \frac{\partial \Gamma_0}{\partial c_0} \frac{\partial^2 c}{\partial r^2} = \mp D \frac{\partial c}{\partial z} \quad \text{at} \quad z = \frac{h}{2} \qquad \text{(surface mass balance)} \qquad (4.2)$$

where c denotes surfactant concentration, r and z are cylindrical coordinates, D and D_s are the bulk and surface diffusion coefficients, v_r is the radial component of the mean mass velocity. The three terms in Eqn (4.2) correspond to convection, surface diffusion and bulk diffusion. The ratio of the last two terms yields

$$\frac{\text{surface diff. flux}}{\text{bulk diff. flux}} \approx D_s \frac{\partial \Gamma_0}{\partial c_0} \frac{\partial^2 c}{\partial r^2} \Big/ \left(D \frac{\partial c}{\partial z} \right) \approx D_s \frac{\partial \Gamma_0}{\partial c_0} \frac{1}{R} \frac{\partial c}{\partial r} \Big/ \left(\frac{Dh}{R} \frac{\partial c}{\partial r} \right) \approx D_s \frac{\partial \Gamma_0}{\partial c_0} / (Dh) \; >> \; 1$$

To get the last estimate we used typical parameters values. Hence one can conclude that in most cases the bulk diffusion plays a negligible role and the surfactant behaves as insoluble.

Another basic equation stems from the *surface momentum balance* relating the stresses exerted on the surfactant adsorption monolayer. The shadowed areas in Fig. 8 depict two consecutive positions of a surface material element at time moments t and $t+dt$. In general, such an element is subjected to both *shear* and *dilatational* deformations. Correspondingly, the surface viscous stress, τ_s, is a superposition of shear, τ_{sh}, and dilatational, τ_{dl}, surface viscous stresses:

$$\tau_S = \tau_{sh} + \tau_{dl} = \left(\eta_{sh} + \eta_{dl}\right) \frac{\partial v_r}{\partial r} \equiv \eta_S \frac{\partial v_r}{\partial r}; \qquad \eta_S \equiv \eta_{sh} + \eta_{dl} \tag{4.3}$$

where η_{sh} and η_{dl} denote the surface shear and dilatational viscosities. The balance of all stresses exerted at the surface element reads [9]:

$$\eta\left(\frac{\partial v_r}{\partial z}\right) = \eta^d\left(\frac{\partial v_r^d}{\partial z}\right) + \frac{\partial \sigma_o}{\partial c_o}\frac{\partial c}{\partial r} + \eta_S \frac{\partial^2 v_r}{\partial r^2} \tag{4.4}$$

where η denotes bulk viscosity and the subscript "*d*" denotes properties of the droplet phase. The four terms in Eqn (4.4) respectively account for the action of the following stresses: viscous friction with the film phase, viscous friction with the droplet phase, surface elastic stress (Marangoni effect), and surface viscous stress. Taking the ratio of the last two terms one obtains

$$\frac{\text{surf. visc. stress}}{\text{surf. elast. stress}} \sim \frac{\eta_S\left(\partial^2 v_r / \partial r^2\right)}{\left(\partial \sigma_0 / \partial c_0\right)\left(\partial c / \partial r\right)} \sim \frac{\eta_S}{E_G R^2 / D_S} \approx \frac{\eta_S}{20 \times (10^{-2})^2 / 10^{-4}} \approx \frac{\eta_S}{20} << 1 \tag{4.5}$$

where at the last steps typical parameters values are substituted;

$$E_G = -A\frac{\partial \Gamma}{\partial A} \tag{4.6}$$

is the Gibbs elasticity of the surfactant adsorption monolayer with A being the interfacial area. From the above estimate one sees that the effect of surface viscosity, η_s, on the drainage of plane-parallel liquid films is negligible.

On the other hand, if smaller droplet may interact like almost non-deformable spheres ($R \to 0$), cf. Fig. 3 above. Setting formally $R \to 0$ in Eqn (4.5) one sees that the contribution of the surface viscosity can be important for the interaction between small droplets. In other words, the effect of the true surface viscosity depends strongly on the length scale.

Below we present the predictions of the theory for the velocity of thinning of emulsion films depending on whether the surfactant is soluble in the continuous or the drop phase.

4.2. Surfactant soluble in the continuous phase (System I)

When the surfactant is soluble in the *continuous* phase (we will call such a system "System I"), the Marangoni effect becomes operative (Fig. 7) and the rate of film thinning becomes dependent on the surface (Gibbs) elasticity, E_G, cf. Eqn (4.6). The solution of the problem [9,40,41] gives the following expression for the rate of thinning of symmetrical planar films (of both foam and emulsion type):

$$\frac{V_{\mathrm{I}}}{V_{\mathrm{Re}}} \approx 1 + \frac{1}{\varepsilon_f} \quad , \quad \frac{1}{\varepsilon_f} = \frac{6\eta D_s}{hE_G} \tag{4.7}$$

where, V_I is the rate of thinning of system I, as usual, D_s is the surface diffusion coefficient, h is the film thickness, and ε_f is the so called *foam parameter* [39]. Note that the surface diffusion flux, which tends to restore the uniform adsorption monolayers, damps the surface tension gradients (which oppose the film drainage) and thus accelerates the film thinning. However, at large surfactant concentrations the surface elasticity, E_G, prevails, ε_f increases, and consequently, the thinning rate decreases down to the Reynolds velocity, $V \to V_{\mathrm{Re}}$, cf. Eqn (4.7). The latter equation predicts that *System I* behaves as a foam system: the rate of thinning is not affected by the circulation of liquid in the droplets. Similar expressions for the rate of film thinning, which are appropriate for various ranges of values of the interfacial parameters, can be found in the literature [9,29,30,31,42,43].

4.3. Surfactant soluble in the drop phase (System II)

Traykov and Ivanov [41] established (both theoretically and experimentally) the interesting effect that when the surfactant is dissolved in the *disperse* phase, that is in the emulsion droplets, they approach each other just like in the case of pure liquid phases:

$$\frac{V_{\mathrm{II}}}{V_{Re}} \approx \frac{1}{\varepsilon^e} \approx \frac{\eta\delta}{\eta^d h} \approx \left(\frac{108\pi\eta^3 R^4}{\rho^d \eta^d h^4 F_z} \right)^{1/3} \tag{4.8}$$

We will call such a system "System II". Here V_{II} is the velocity of thinning for System II, and δ is the thickness of the hydrodynamic boundary layer inside the drops and ρ^d is the density of the drop phase. Qualitatively, this effect can be attributed to the fact that the convection driven surface tension gradients are rapidly damped by the influx of surfactant from the drop interior (see Fig. 9); in this way the Marangoni effect is suppressed. Indeed, during the film drainage the surfactant is carried away toward the film border and a non-equilibrium distribution, depicted in Fig. 7, appears. Since however the mass transport is proportional to the perturbation, the larger the deviation from equilibrium, the stronger the flux tending to eliminate the perturbation (the surfactant flux is denoted by thick arrows in Fig. 9). In this way any surface concentration gradient (and the related Marangoni effect) disappears. The emulsion films in this case behave as if surfactant is absent.

4.4. Comparison of System I and System II; demulsification

Sketch of Systems I and II is presented in Fig. 10. The surfactant is assumed to be soluble in Liquid 1 and insoluble in Liquid 2. As seen in Fig.10, the difference between Systems I and II consists in the exchanged continuous and the drop phases.

Assume for simplicity that V_{Re} for both systems is the same. In addition, usually $\varepsilon_f \approx 0.1$ and $\varepsilon_e \approx 10^{-2} - 10^{-3}$. Then from Eqns (4.7) and (4.8) one obtains

$$\frac{V_{\mathrm{II}}}{\mathrm{V_I}} \approx \frac{\varepsilon^f}{\varepsilon^e} \approx \frac{0.1}{10^{-2} \text{ to } 10^{-3}} \approx 10 \text{ to } 100 \tag{4.9}$$

Hence, the rate of film thinning in System I is much greater than that in System II. Therefore, the location of the surfactant has a dramatic effect on the thinning rate and thereby--on the drop life time. The mere phase inversion of an emulsion A/B to B/A, may change the emulsion life time by orders of magnitude. This fact is closely related to the explanation of the Bancroft rule for the stability of emulsions (see below). This fact also helps for the understanding of the process of chemical demulsification.

It is known [44] that one way to destroy an emulsion is to add a surfactant, which is soluble in the drop phase – this method is termed *chemical demulsification*. To understand the underlying process let us consider two colliding emulsion droplets with film formed in the zone of collision, cf. Fig10. As discussed above, when the liquid is flowing out of the film, the viscous drag exerted on the film surfaces (from the side of the film interior) carries away the adsorbed emulsifier toward the film periphery. Thus a non-uniform surface distribution of the emulsifier (shown in Fig. 11a by empty circles) is established. If demulsifier (the full circles in Fig. 11b) is present in the drop phase, it will occupy the interfacial area freed by the emulsifier. The result will be a saturation of the adsorption layer, as shown in Fig. 11b. If the demulsifier is sufficiently surface active, its molecules will be able to substantially decrease, and even to completely eliminate, the interfacial tension gradients thus turning the emulsion to type II, see Fig. 10. This leads to a strong increase in the rate of film thinning, rapid drop coalescence and emulsion destruction. The above mechanism suggests that the demulsifier has to possess the following properties [17]:

(i) It must be soluble in the drop phase or in both phases, but in the latter case its solubility in the drop phase must be much higher.

(ii) Its diffusivity and concentration must be large enough to provide a sufficiently large demulsifier flux toward the surfaces and thus to eliminate the gradients of the interfacial tension.

(iii) Its surface activity must be comparable and even higher than that of the emulsifier. Otherwise, even though it may adsorb, it will not be able to suppress the interfacial tension gradients.

5. Factors affecting the thermodynamic stability of emulsion films

Below we discuss new results about two thermodynamic stabilizing factors most frequently appearing in practice: the electrostatic and oscillatory structural forces.

5.1. Electrostatic effects

First of all we have to note that the interface between *pure* oil and water phases (in the absence of any surfactants) bears a considerable negative surface potential; the measured ζ-potential of oil droplets in water is of the order of -60 mV. This has been first established by Carruthers [45] who measured the electrophoretic mobility of octadecane droplets and established a pronounced pH-dependence of the ζ-potential. Similar experiments have been carried out by Dickinson [46], Taylor and Wood [47], Marinova et al. [48]. These authors conclude that the negative surface potential can be attributed to the adsorption of hydroxyl ions from the water to the water-oil interface. It is worthwhile noting that ζ-potentials of similar sign and magnitude have been measured also with air bubbles in water [49,50]. The charge of the air-water interface is high enough to be able to stabilize in some cases free aqueous films without any surfactant [51].

Considerable surface potentials have been detected also with oil-water interfaces in the presence of *nonionic* surfactants, whose molecules are not ionizable [52,53]. An example is given in Fig. 12, where data from Ref. [54] for the ζ-potential of oil droplets for mixtures of Tween (water soluble) and Span (oil soluble) are plotted vs. the mole fraction of the mixture. One sees that the ζ-potential decreases with the increase of the concentration of Tween. Possible explanations can be that (i) the Tween displaces the surface charges from the oil-water interface, or (ii) the dipole moment of Tween creates a surface potential with sign opposite to that of the bare oil-water interface. Anyway, this relatively high surface potential was found to contribute to a considerably longer life-time of emulsion drops released against flat homophase in the presence of Span-Tween blends [13].

Another effect of electrostatic origin, which contributes to the stabilization of emulsions, is the short-range monotonic *hydration repulsion* [55]. It is most pronounced when strongly hydrated counterions, such as Mg^{2+} and Li^{+} are present in the solution. The resulting short-range repulsion can be attributed to the volume excluded by the hydrated counterions in the vicinity of the interface [56]; in other words, the hydrated counterions for a protective shell around the emulsion droplets, which impedes their flocculation and coalescence upon collision.

5.2. Oscillatory structural forces

In general, oscillatory structural forces appear in two cases: (i) in thin films of pure solvent between two smooth *solid* surfaces; (ii) in thin liquid films containing colloidal particles (including macromolecules and surfactant micelles). In the first case the oscillatory forces are

called the "solvation forces" [55,57]; they could be important for the short-range interactions between solid particles in dispersions. In the second case, the structural forces affect the stability of foam and emulsion films as well as the flocculation processes in various colloids. At higher particle concentrations the structural forces stabilize the liquid films and colloids [58-67], see Fig. 13. At lower particle concentrations the structural forces degenerate into the so called *depletion attraction*, which is found to destabilize various dispersions [68,69].

In the special case of emulsions the maxima (Fig. 14) of the oscillatory disjoining pressure (just like the electrostatic maximum in Fig. 6) act like barriers against the closer approach and flocculation (or coalescence) of the droplets [3]. These maxima are high enough to affect the flocculation when the particle (micelle) volume fraction, is greater than c.a. 20% of the continuous phase. This is often the experimental situation when a mixture of surfactants is used to stabilize the emulsion: the micellisation synergistic effects increase the micelle volume fraction thus enhancing the stabilization effect of the oscillatory structural forces.

Henderson [70] derived an explicit (though rather complex) formula for calculating the oscillatory structural forces. Numerical simulations [71,72] and density-functional modeling [73] of the step-wise thinning of foam films are also available.

Recently, a semiempirical formula for the oscillatory structural component of disjoining pressure was proposed [74]

$$\Pi_{osc}(h) = P_0 \cos\left(\frac{2\pi h}{d_1}\right) \exp\left(\frac{d^3}{d_1^2\, d_2} - \frac{h}{d_2}\right) \qquad \text{for } h > d$$
$$= -P_0 \qquad \text{for } 0 < h < d \tag{5.1}$$

where d is the diameter of the hard spheres, d_1 and d_2 are the period and the decay length of the oscillations which are related to the particle volume fraction, φ, as follows [74]

$$\frac{d_1}{d} = \sqrt{\frac{2}{3}} + 0.237\,\Delta\varphi + 0.633(\Delta\varphi)^2\,; \qquad \frac{d_2}{d} = \frac{0.4866}{\Delta\varphi} - 0.420 \tag{5.2}$$

Here $\Delta\varphi = \varphi_{max} - \varphi$ with $\varphi_{max} = \pi/(3\sqrt{2})$ being the value of φ at close packing. P_0 is the particle osmotic pressure determined by means of Carnahan-Starling formula [75]

$$P_0 = n\,k\,T\,\frac{1+\varphi+\varphi^2-\varphi^3}{(1-\varphi)^3}, \qquad n = \frac{6\varphi}{\pi d^3}, \tag{5.3}$$

where n is the particle number density. For $h < d$, when the particles are expelled from the slit into the neighboring bulk suspension, Eqn (5.1) describes the *depletion attraction*. On the other hand, for $h > d$ the structural disjoining pressure , Π_{osc}, oscillates around P_0 (defined by Eqn 5.3) in agreement with the finding of Kjellander and Sarman [76]. The contribution of the oscillatory

structural forces to the interaction free energy per unit area of the film can be obtained by integrating Π_{osc}:

$$f_{osc}(h) = \int_{h}^{\infty} \Pi_{os}(h')\, dh' \tag{5.4}$$

It should be noted that Eqns (5.1) - (5.3) refer to hard spheres of diameter d. In practice, however, the interparticle potential can be "soft" because of the action of some long-range forces. In the case of charged particles, like ionic surfactant micelles, the following approximate expression can be also used [65]

$$d = d_{\mathrm{H}} + 2\kappa^{-1} \tag{5.5}$$

where d_{H} is the hydrodynamic diameter of the particle, determined, say, by dynamic light scattering. It was found [65,74] that Eqn (5.5) compares well with the experimental data for stratifying films.

As an illustration let us consider recent experimental data [77] for micellar solutions of the ionic surfactant *sodium nonylphenol polyoxyethylene-25 sulfate* (SNP-25S) at concentration 3.35×10^{-2} M. The step-wise thinning of a film formed from such a micellar solution is shown in Fig. 13. This step-wise thinning, called stratification, is due to the oscillatory structural forces caused by the presence of spherical surfactant micelles in the solution [58]. Comparative experiments with 0.1 M added NaCl and without any added NaCl have been carried out [77]. From the experimental number concentration of the micelles, n, their effective diameter, d, and volume fraction, φ, have been calculated by means of Eqns (5.3) and (5.5) and listed in Table 1 One sees that the addition of 0.1 M electrolyte (NaCl) decreases the volume fraction of the micelles from 0.32 to 0.18 due to the shrinkage of the micelle counterion atmospheres. The period and decay length of the oscillations, d_1 and d_2 , are calculated from Eqn (5.2); one sees that d_2 is markedly lower than d_1 and d, especially for the lower volume fraction φ=0.18. The electrostatic and van der Waals surface free energies, f_{el} and f_{vw}, are calculated by means of the DLVO theory [5] with Hamaker constant $A_{\mathrm{H}} = 5\times10^{-21}$ J and area per surface charge 76 Å^2, whereas, the oscillatory free energy, f_{osc}, is determined from Eqns (5.1) and (5.4). The experimental values of the contact angle, θ, of the respective films are also shown in Table 1. The theoretical values of θ are calculated by means of the expression [78]

$$f = f_{el} + f_{vw} + f_{osc} = -2\sigma(1 - \cos\theta) \tag{5.6}$$

with σ=7.5 mN/m. One sees that the theoretical and the experimental values of θ coincide in the framework of the experimental accuracy [77]. The theoretical plot of f_{osc} vs. h calculated by means of Eqns (5.1) and (5.4) with the parameters values taken from Table 1 is shown in Fig. 14. Note that the experimental thickness of the film containing one layer of surfactant micelles

corresponds to the first minimum of f_{osc} (that at $h \approx 12$ nm in Fig. 14). In general, the *metastable* states of the film (the steps in Fig. 13) correspond (approximately) to the *minima* of f vs h curve.

Table 1. Data for stratifying films stabilized by SNP-25S at concentration 3.35×10^{-2} M, [77].

C_{el} M NaCl	φ	d nm	d_1 nm	d_2 nm	f_{el} (10^{-3} erg /cm^2)	f_{vw} (10^{-3} erg /cm^2)	f_{osc} (10^{-3} erg /cm^2)	θ theory deg	θ experim. deg
0.1	0.18	7.7	8.8	3.4	0.03	–0.40	–1.85	0.98	1.0±0.04
0	0.32	9.3	9.5	7.0	5.20	–0.37	–13.43	1.94	1.89±0.08

The numerical results in Table 1 show that in the system under consideration the contribution of the oscillatory structural force, f_{osc}, to the total surface free energy, f, is the greatest one, cf. Eqn (5.6). Moreover, the magnitude of f_{osc} (the depth of the first minimum in Fig. 14) increases with the decrease of the electrolyte concentration because of the increase of the micelle effective volume fraction φ. As a result, the contact angle, θ, increases with the decrease of electrolyte concentration. This tendency is exactly the opposite to that in the absence of micelles (surfactant concentrations around and below CMC), when oscillatory structural forces are missing.

6. Theoretical interpretation of the Bancroft rule for emulsions

As discussed above, the stability of emulsions is determined by an interplay of hydrodynamic forces (related to the Gibbs elasticity, bulk viscosity, surface diffusion, etc.) and the disjoining pressure, which may be due to DLVO forces, oscillatory structural forces, etc. Our aim below is to formulate a general (though approximate) criterion for emulsion stability, which accounts adequately for the role of the various factors.

Historically, the first attempt to formulate simple rules connecting the emulsion stability with the surfactant properties was the *Bancroft rule* [79]. It states that "in order to have a stable emulsion the surfactant must be soluble in the continuous phase". A more sophisticated criterion was proposed by Griffin [80] who introduced the concept of the Hydrophilic-Lipophilic Balance (HLB). As far as emulsification is concerned, surfactants with HLB-number in the range 3-6 must form water in oil (W/O) emulsions, whereas those with HLB-numbers 8-18 are expected to form oil in water (O/W) emulsions. Schinoda and Friberg [81] proved that the HLB-number is not a property of the surfactant molecules only, but it also depends strongly on the temperature

(for non-ionic surfactants), on the type and the concentration of added electrolytes, on the type of oil phase, etc. They proposed to use the phase inversion temperature (PIT) instead of HLB for characterization of the emulsion stability. Davis [82] summarized the concepts about HLB, PIT and Windsor's ternary phase diagrams for the case of *microemulsions* and reported topological ordered models, connected with the Helfrich membrane bending energy.

We have proposed [17,83] a semi-quantitative theoretical approach that provides a straightforward explanation of the Bancroft rule for emulsions. This approach is based on the idea of Davies and Rideal [44] that both types of emulsions are formed during the homogenization process, but only the one with lower coalescence rate survives. If the initial drop concentration for both emulsions is the same, the coalescence rates for the two emulsions, $(\text{Rate})_{\text{I}}$ for System I and $(\text{Rate})_{\text{II}}$ for System II (see Fig. 10), will be (approximately) proportional to the respective velocities of film thinning, V_{I} and V_{II}:

$$\frac{(\text{Rate})_{\text{I}}}{(\text{Rate})_{\text{II}}} \approx \frac{V_{\text{I}}}{V_{\text{II}}} \tag{6.1}$$

Using Eqns (1.1), (2.1), (4.7), and (4.8) one can transform Eqn (6.1) to read

$$\frac{(\text{Rate})_{\text{I}}}{(\text{Rate})_{\text{II}}} \approx \underbrace{(486\rho^d D_s^3)^{1/3}}_{8.5\times10^{-4}} \underbrace{\left(\frac{h_{cr,\text{I}}^3}{h_{cr,\text{II}}^2}\right)^{1/3}}_{1.8\times10^{-2}} \underbrace{\left(\frac{\eta^d}{R^2}\right)^{1/3}}_{5} \frac{P_c - \Pi_{\text{I}}}{E_G\left(P_c - \Pi_{\text{II}}\right)^{2/3}} \tag{6.2}$$

where $h_{cr,\text{I}}$ and $h_{cr,\text{II}}$ denote the critical thickness of film rupture for the two emulsions in Fig. 10; values of the multipliers in the right-hand side of Eqn (6.2) for typical parameter values are shown below Eqn. (6.2). In fact, the first three multipliers in Eqn (6.2) are related to the *hydrodynamic* stability, whereas the last multiplier accounts for the *thermodynamic* stability of an emulsion film. Many conclusions can be drawn from Eqn (6.2), regarding the type of emulsion to be formed:

(i) If the disjoining pressures, Π_{I} and Π_{II}, are zero (thick films) the ratio in Eqn (6.2) will be very small. Hence emulsion I (surfactant soluble in the continuous phase) will coalesce much more slowly and it will survive. This underlines the crucial importance of the *surfactant location* (which is connected with its solubility) thus providing a theoretical foundation of Bancroft's rule. The emulsion behavior in this case will be controlled almost entirely by the hydrodynamic factors (*kinetic stability*).

(ii) The *disjoining pressure*, Π, plays an important role. It can substantially change and even reverse the behavior of the system if it is comparable by magnitude with the capillary pressure, P_c. For example if $(P_c - \Pi_{\text{II}}) \to 0$ at finite value of $P_c - \Pi_{\text{I}}$ (which may happen e.g. for O/W emulsion with oil soluble surfactant) the ratio in Eqn (6.2) may become much larger than unity, which means that System II will become *thermodynamically stable*. In some cases the

stabilizing disjoining pressure is large enough for emulsions of very high volume fraction of the disperse phase (above 95% in some cases) to be formed [84].

(iii) The *Gibbs elasticity*, E_G, favors the formation of emulsion I, because it slows down the film thinning. On the other hand, increased *surface diffusivity*, D_s, decreases this effect, because it helps the interfacial tension gradients to relax thus facilitating the formation of emulsion II, cf. Fig. 10.

(iv) The *film radius*, R, increases and the capillary pressure, $P_c = 2\sigma / R_d$, decreases with the drop radius, R_d. Therefore, larger drops will tend to form emulsion I, although the effect is not very pronounced.

(v) The difference between the *critical thicknesses* of the two emulsions affects only slightly the rate ratio in Eqn (6.2), although the value of h_{cr} itself is important.

(vi) The *viscosity* of the continuous phase, η, has no effect on the rate ratio which depends only slightly on the viscosity of the drop phase, η^d. This is in agreement with the experimental observations, see Ref. [44], p. 381 therein.

(vii) The *interfacial tension,* σ, affects the rate ratio directly only through the capillary pressure, $P_c = 2\sigma/R_d$. The *electrolyte* affects most of all the electrostatic disjoining pressure, Π, which decreases as the salt content increases, thus destabilizing the O/W emulsion. It can also influence the stability by changing the surfactant adsorption (including the case of non-ionic surfactants).

(viii) The *temperature* affects strongly (1) the solubility and (2) the surface activity of non-ionic surfactants [85]. It is well known that at higher temperature non-ionic surfactants become more oil-soluble, which favors the W/O emulsion. Thus effect (1) may change the type of emulsion formed at the Phase Inversion Temperature (PIT). Effect (2) has numerous implications, the most important being the change of the Gibbs elasticity, E_G, and the interfacial tension, σ.

(ix) *Surface active additives* (cosurfactants, demulsifiers, etc.), such as fatty alcohols in the case of ionic surfactants, may affect the emulsifier partitioning between the phases and its adsorption, thereby changing the Gibbs elasticity and the interfacial tension. The surface active additive may change also the surface charge (mainly by increasing the spacing among the emulsifier ionic headgroups) thus decreasing the repulsive electrostatic disjoining pressure and favoring the W/O emulsion. Polymeric surfactants and adsorbed proteins increase the steric repulsion between the film surfaces. They may favor either of the emulsions O/W or W/O depending on their conformation at the interface and their surface activity.

(x) The *interfacial bending moment,* B_0, can also affect the type of the emulsion, although this is not directly visible from Eqn (6.2). Note that $B_0 = -4k_c H_0$, where H_0 is the so called

spontaneous curvature and k_c is the interfacial curvature elastic modulus [86]; typically B_0 is of the order of 5×10^{-11} N [87]. For O/W emulsions B_0 usually opposes the flattening of the droplet surfaces in the zone of collision (Fig. 10), but for W/O emulsions B_0 favors the flattening [3]. Indeed, the expression for the curvature contribution in the energy of droplet-droplet interaction reads [3]:

$$W_c = -2\pi R^2 B_0 / R_d, \qquad (R / R_d)^2 << 1 \tag{6.3}$$

It turns out that $W_c > 0$ for the droplet collisions in an O/W emulsion, while $W_c < 0$ for a W/O emulsion [3]; consequently the interfacial bending moment stabilizes the O/W emulsions, but destabilizes the W/O ones. There is supporting experimental evidence [88] for dimerisation in W/O microemulsions. The effect of the bending moment can be important even for droplets of μm size, see Ref. [3].

7. Stability of emulsions from non-preequilibrated phases

All conclusions drawn in the previous section are valid for emulsions formed from preequilibrated phases. We describe below some recent results showing that interesting phenomena happen in emulsion films formed from non-preequilibrated phases. These phenomena can prevent the film rupture for a period from hours to days, even though the film is thermodynamically unstable. This kinetic source of stability represents not only academic, but also practical interest, in so far as non-preequilibrated emulsions are often used in the technological processes.

The common non-ionic surfactants are often soluble in both water and oil phases. Let us consider the case when the surfactant (the emulsifier) is initially dissolved in one of the liquid phases and then the emulsion is prepared by homogenization. In such a case, the initial distribution of the surfactant between the two phases of the emulsion is a non-equilibrium one. Therefore, surfactant diffusion fluxes appear across the surfaces of the emulsion droplets. The process of surfactant redistribution usually lasts from several hours to several days, until finally equilibrium distribution is established. The diffusion fluxes across the interfaces, directed either from the continuous phase toward the droplets or contrariwise, are found to stabilize both thin films and emulsions. If the films are thermodynamically unstable, they may exist several hours (up to days) because of the diffusion surfactant transfer; however, they rupture immediately after the diffusive equilibrium has been established. Experimentally this effect manifests itself in phenomena called *cyclic dimpling* [89] and *osmotic swelling* [90]. These two phenomena are described and discussed below.

7.1. Surfactant transfer from continuous to disperse phase (cyclic dimpling)

The phenomenon cyclic dimpling was first oserved [89] with xylene films intervening between two water droplets in the presence of the non-ionic emulsifier Tween 20 or Tween 80 (initially dissolved in water, but also soluble in oil). The same phenomenon has been observed also with other emulsion systems.

After the formation of such an emulsion film, it thins down to a quasi-equilibrium thickness (c.a. 100 nm), determined mostly by the electrostatic repulsion between the interfaces. As soon as the film reaches this thickness, a dimple spontaneously forms in the film center and starts growing (Fig. 15a). When the dimple becomes bigger and approaches the film periphery, a channel forms connecting the dimple with the aqueous phase outside the film (Fig. 15b). Then the water solution contained in the dimple flows out leaving an almost plane-parallel film behind. Just afterwards a new dimple starts to grow and the process repeats again. The period of this cyclic dimpling remains approximately constant for many cycles and could be from a couple of minutes up to more than ten minutes. It was established [89,91] that this process is driven by the depletion of the surfactant concentration in the central zone of the film surfaces due to the dissolving and diffusion of surfactant in the adjacent oil phases (Fig. 15a). The gradient of the surfactant adsorption gives rise to a surface tension gradient, which triggers a surface convective flux along the two film surfaces directed from the periphery toward the center. The tangential movement of the film surfaces drags along a convective influx of solution in the film, which feeds the dimple. Thus the cyclic dimpling appears to be a process leading to stabilization of the emulsion films and emulsions due to the influx of additional liquid in the region between the droplets which prevents them from a closer approach, and eventually, from coalescence.

Combining the general equation for films with mobile surfaces one can derive [91]

$$\frac{\partial h}{\partial t}+\frac{1}{3\eta r}\frac{\partial}{\partial r}\left\{rh^3\frac{\partial}{\partial r}\left[\frac{\sigma}{r}\frac{\partial}{\partial r}\left(r\frac{\partial h}{\partial r}\right)+\Pi(h)\right]\right\}=\frac{1}{2r}\frac{\partial}{\partial r}\left(\frac{j\,h\,r^2}{\Gamma}\right) \tag{7.1}$$

where j is the diffusion flux in the drop phase, and as usual, r is radial coordinate, $h(r,t)$ is the film thickness, σ is surface tension, Γ is adsorption, and Π is disjoining pressure. The comparison between the numerical calculations based on Eqn (7.1) and the experimental data for the cyclic dimpling show a very good quantitative agreement [91].

7.2. Surfactant transfer from disperse to continuous phase (osmotic swelling)

Velev *et al*. [13] reported that emulsion films, formed from preequilibrated phases containing the non-ionic surfactant Tween and 0.1 M NaCl, spontaneously thin down to Newton Black Films (thickness ≈ 10nm), and then rupture. However, when the non-ionic surfactant Tween 20 or Tween 60 is initially dissolved in the xylene drops and the film is formed from the

non-preequilibrated phases, no black film formation and rupture is observed [90]. Instead, the films have a thickness above 100 nm, and one observes formation of channels of larger thickness connecting the film periphery with the film center (Fig. 16). One may observe that the liquid is circulating along the channels for a period from several hours to several days. The phenomenon continues until the redistribution of the surfactant between the phases is accomplished. This phenomenon occurs only when the background surfactant concentration in the continuous (the aqueous) phase is larger than CMC. These observation can be interpreted in the following way.

Since the surfactant concentration in the oil phase (the disperse phase) is higher than the equilibrium one, surfactant molecules cross the oil-water interface toward the aqueous phase. In so far as the background surfactant concentration in the aqueous phase is not less than CMC, the excess surfactant present in the film is packed in the form of micelles (denoted by black dots in Fig. 16a). Thus surfactant micelles accumulate within the film, because the diffusion of micelles throughout the film is not fast enough to promptly transport the excess of surfactant into the Plateau border. As a consequence the film is subjected to *osmotic swelling* because of the excess concentration of micelles, ΔC_{mic}, within. The excess osmotic pressure

$$P_{\mathrm{osm}} = kT\,\Delta C_{\mathrm{mic}} \geq P_c \tag{7.2}$$

counterbalances the outer capillary pressure and arrests the further thinning of the film. Moreover, the excess osmotic pressure in the film gives rise to a convective outflow of solution through the channels (Fig. 16b).

The experiment [90] shows that the occurrence of the above phenomenon is the same for initial surfactant concentration in the water varying from 1 up to 500 times the CMC, if only some amount of surfactant is initially dissolved also in the oil. This fact implies that the value of the surfactant chemical potential inside the oil phase is much greater than that of the surfactant monomers in the aqueous phase, the latter being always close to its value at the CMC in the investigated range of concentrations.

8. Concluding remarks

In summary, the major *thermodynamic* factors influencing the emulsion stability are the temperature and the disjoining pressure. The latter can be due to the DLVO forces (double layer repulsion and van der Waals attraction), as well as to various non-DLVO surface forces such as the hydration repulsion, ionic correlation forces, oscillatory structural forces, hydrophobic attraction, steric polymer adsorption forces, fluctuation wave forces (protrusion, undulation, etc.), see Refs. [55,92,15,31].

In addition, an important role is played also by the *hydrodynamic* forces related to the bulk viscosity of the liquid phases and bulk diffusion; surface viscosity of the surfactant

adsorption monolayers and surface diffusion; surface (Gibbs) elasticity (Marangoni effect) and thermoelasticity; droplet deformability and bending energy; solubility of the surfactant in the water and oil phases and the presence of surfactant transfer across the phase boundaries.

An interplay of many factors, of both thermodynamic and hydrodynamic origin, takes place in the real emulsion systems, which therefore seem to be a practically inexhaustible research field. Eqn (6.2) above represents an attempt to quantify the contributions of the major factors thus helping to formulate a special "diagnosis" for the stability of each separate emulsion system.

Acknowledgment: This study was supported in part by Kraft General Foods, Inc., and in part by the Bulgarian National Science Fund.

REFERENCES

1. K.D. Danov, D.N. Petsev, N.D. Denkov and R. Borwankar, *J. Chem. Phys.,* 99 (1993) 7179.
2. K.D. Danov, N.D. Denkov, D.N. Petsev and R. Borwankar, *Langmuir,* 9 (1993) 1731.
3. D.N. Petsev, N.D. Denkov and P.A. Kralchevsky, *J. Colloid Interface Sci.,* 176 (1995) 201.
4. B.V. Derjaguin, *Kolloid Zeits.,* 69 (1934) 155.
5. B.V. Derjaguin, N.V. Churaev and V.M. Muller, Surface Forces*,* Plenum Press: Consultants Bureau, New York, 1987.
6. E.D. Shchukin, A.V. Pertsov and E.A. Amelina, Colloid Chemistry*,* Moscow Univ. Press, Moscow, 1982 [in Russian].
7. O. Reynolds, *Phil. Trans. Roy. Soc. (London)* A177 (1886) 157.
8. A. Scheludko, *Adv. Colloid Interface Sci.* 1 (1967) 391.
9. I.B. Ivanov and D.S. Dimitrov, in: Thin Liquid Films (I.B. Ivanov, ed.), M. Dekker, New York, 1988, p. 379.
10. N.D. Denkov, D.N. Petsev, and K.D. Danov, *J. Colloid Interface Sci.* 176 (1995) 189.
11. P. Taylor, *Proc. Roy. Soc. (London)* A108 (1924) 11.
12. R. Aveyard, B.P. Binks, P. Fletcher and X. Ye, *Prog. Colloid Polymer Sci.,* 89 (1992) 114.
13. O.D. Velev, T.D. Gurkov,S.K. Chakarova, B. Dimitrova and I.B. Ivanov, *Colloids Surfaces A* 83 (1994) 43.
14. S.S. Davis and A. Smith, *Colloid Polym. Sci.,* 254 (1976) 82.
15. P.A. Kralchevsky, K.D. Danov and N.D. Denkov, in: Handbook of Surface and Colloid Chemistry, CRC Press, London, 1996.

16. E. Dickinson, B.S. Murray and G. Stainsby, *J. Chem. Soc. Faraday Trans.* 84 (1988) 871.

17. I.B. Ivanov, Lectures at INTEVEP, Petroleos de Venezuela, Caracas, June 1995.

18. A. Scheludko, *Proceedings Koninkl. Ned. Akad. Wet., Amsterdam,* B65 (1962) 76.

19. K.J. Mysels, *J. Phys. Chem.*, 68 (1964) 3441.

20. O.D. Velev, G.N. Constantinides, D.G. Avraam, A.C. Payatakes and R.P.Borwankar, *J. Colloid Interface Sci.* 175 (1995) 68.

21. S.G. Yiantsios and R.H. Davis, *J. Colloid Interface Sci.* 144 (1991) 412.

22. S.G. Yiantsios and B.G. Higgins, *J. Colloid Interface Sci.* 147 (1991) 341.

23. J.-L. Joye, G.J. Hirasaki and C.A. Miller, *Langmuir* 8 (1992) 3085.

24. J.-L. Joye, G.J. Hirasaki and C.A. Miller, *Langmuir* 10 (1994) 3174.

25. S. Frankel and K. Mysels, *J. Phys. Chem.* 66 (1962) 190.

26. B.K. Chi and L.G. Leal, *J. Fluid Mech.* 201 (1989) 123.

27. E.P. Ascoli, D.S. Dandy and L.G. Leal, *J. Fluid Mech.* 213 (1990) 287.

28. S.G. Yiantsios and R.H. Davis, *J. Fluid Mech.* 217 (1990) 547.

29. D. Li, *J. Colloid Interface Sci.* 163 (1994) 108.

30. I.B. Ivanov, D.S. Dimitrov, P. Somasundaran and R.K. Jain, *Chem. Eng. Sci.* 40 (1985) 137.

31. P.A. Kralchevsky, K.D. Danov and I.B. Ivanov, Thin Liquid Film Physics, in: *Foams: Theory, Measurements and Applications*, R.K. Prud'homme, Ed.; M. Dekker, New York, 1995, p.1.

32. D. Exerowa, A. Nikolov and M. Zacharieva, *J. Colloid Interface Sci.* 81 (1981) 419.

33. A.J. de Vries, *Rec. Trav. Chim. Pays-Bas.* 77 (1958) 441.

34. A. Vrij, *Discuss. Faraday Soc.* 42 (1966) 23.

35. I.B. Ivanov, B.P. Radoev, E.D. Manev and A.D. Sheludko, *Trans. Faraday Soc.* 66 (1970) 1262.

36. C. Maldarelli, R.K. Jain, I.B. Ivanov and E. Ruckenstein, *J. Colloid Interface Sci.* 78 (1980) 118.

37. C. Maldarelli and R.K. Jain, "The Hydrodynamic Stability of Thin Films" in: *Thin Liquid Films*, I.B. Ivanov, Ed., M. Dekker, New York, 1988, p. 497.

38. I.B. Ivanov and D.S. Dimitrov, *Colloid Polym. Sci.* 252 (1974) 982.

39. I.B. Ivanov, *Pure Appl. Chem.* 52 (1980) 1241.

40. D.S. Dimitrov and I.B. Ivanov, *J. Colloid Interface Sci.* 64 (1978) 97.

41. T.T. Traykov and I.B. Ivanov, *Int. J. Multiphase Flow* 3 (1977) 471.

42. C.-Y.D. Lu and M.E. Cates, *Langmuir* 11 (1995) 4225.

43. S.A.K. Jeelany and S. Hartland, *J. Colloid Interface Sci.* 164 (1994) 296.

44. J. Davies and E. Riedal, Interfacial Phenomena, Academic Press, New York, 1963.

45. J.C. Carruthers, *Trans. Faraday Soc.* 34 (1938) 300.

46. W. Dickinson, *Trans. Faraday Soc.* 37 (1938) 140.

47. A.J. Taylor and F.W. Wood, *Trans. Faraday Soc.* 53 (1957) 523.

48. K.G. Marinova, R.G. Alargova, N.D. Denkov, O.D. Velev, D.N. Petsev, I.B. Ivanov and R.P. Borwankar, *Langmuir* 12 (1996) 2045.

49. H.A. Mctaggart, *Philos. Mag.* 27 (1914) 29.

50. A. Graciaa, G. Morel, P. Saulnier, J. Lashaise and R.S. Schechter *J. Colloid Interface Sci.* 172 (1995) 131.

51. D. Exerowa and M. Zacharieva, in: Research in Surface Forces, Vol.4, B.V. Derjaguin, Ed., Consultants Bureau, New York, 1975.

52. P.H. Elworthy, A.T. Florence and J.A. Rogers, *J. Colloid Interface Sci.* 35 (1971) 23.

53. P. Becher and M.J. Schick, in: Nonionic Surfactants, M.J. Schick, Ed., M. Dekker, New York, 1987.

54. O. Velev, T, Gurkov, R. Alargova, K. Marinova, I. B. Ivanov, R. Borwankar, "Stability of Foams and Emulsions in the Presence of Nonionic Surfactant Blends", in: *Proc. First World Congress on Emulsions*, Paris, October, 1993.

55. J. N. Israelachvili, Intermolecular and Surface Forces, Academic Press, London, 1992.

56. V.N. Paunov, R.I. Dimova, P.A. Kralchevsky, G. Broze, and A. Mehreteab, J. Colloid Interface Sci. 182 (1996) 239.

57. R.G. Horn, and J.N. Israelachvili, *Chem. Phys. Lett.* 71 (1980) 192.

58. A.D. Nikolov, D.T. Wasan, P.A. Kralchevsky, and I.B. Ivanov, in: Ordering and Organisation in Ionic Solutions, N. Ise and I. Sogami, Eds., World Scientific, Singapore, 1988.

59. D.T. Wasan, A.D. Nikolov, P.A. Kralchevsky and I.B. Ivanov, *Colloids Surfaces* 67 (1992) 139.

60. H.G. Bruil and J. Lyklema, *Nature* 233 (1971) 19.

61. S. Friberg, St. E. Linden and H. Saito, *Nature* 251 (1974) 494.

62. P.M. Kruglyakov, *Kolloidn. Zh.* 36 (1974) 160.

63. E. Manev, S.V. Sazdanova and D.T. Wasan, *J. Dispersion Sci. Technol.* 5 (1984) 111.

64. P. Richetti and P. Kekicheff, *Phys. Rev. Lett.* 68 (1992) 1951; ibid., p. 1955.

65. A.D. Nikolov and D.T. Wasan, *J. Colloid Interface Sci.* 133 (1989) 1.

66. E.S. Basheva, A.D. Nikolov, P.A. Kralchevsky, I.B. Ivanov, and D.T. Wasan, in: Surfactants in Solution, Vol. 12, K.L.Mittal and D.O. Shah, Eds., Plenum Press, New York, 1991, p.467.

67. V. Bergeron and C.J. Radke, *Langmuir* 8 (1992) 3020.

68. S. Asakura and F. Oosawa, *J. Chem. Phys.* 22 (1954) 1255; *J. Polym. Sci.* 33 (1958) 183.

69. H. de Hek and A. Vrij, *J. Colloid Interface Sci.* 84 (1981) 409.

70. D. Henderson, *J. Colloid Interface Sci*. 121 (1988) 486.

71. X.L. Chu, A.D. Nikolov and D.T. Wasan, *Langmuir* 10 (1994) 4403.

72. X.L. Chu, A.D. Nikolov and D.T. Wasan, *J. Chem. Phys.* 103 (1995) 6653.

73. M.L. Pollard and C. J. Radke, *J. Chem. Phys.* 101 (1994) 6979.

74. P.A. Kralchevsky and N.D. Denkov, *Chem. Phys. Lett.* 240 (1995) 385.

75. N.F. Carnahan and K.E. Starling, *J. Chem. Phys.* 51 (1969) 635.

76. R. Kjellander and S. Sarman, *Chem. Phys. Lett.* 149 (1988) 102.

77. K.G. Marinova, T.D. Gurkov, T.D. Dimitrova, R.G. Alargova and D. Smith, *Langmuir* (1996) - submitted.

78. J. A. de Feijter, in: Thin Liquid Films, I.B. Ivanov, Ed., M. Dekker, New York, 1988, p.1.

79. W.D. Bancroft, *J. Phys. Chem.* 17 (1913) 514.

80. J. Griffin, *Soc. Cosmet. Chem.* 5 (1954) 4.

81. K. Shinoda and S. Friberg, Emulsions and Solubilization, Wiley, New York, 1986.

82. H.T. Davis, "Factors Determining Emulsion Type: HLB and beyond" in: *Proc. First World Congress on Emulsions,* Paris, 1993, p. 69.

83. K.D. Danov, O.D. Velev, I.B. Ivanov and R.P. Borwankar, "Bancroft Rule and Hydrodynamic Stability of Thin Films and Emulsions" in: *Proc. First World Congress on Emulsions,* Paris, 1993.

84. H. Kunieda, D.F. Evans, C. Solans and Yoshida, *Colloids Surfaces* 47 (1990) 35.

85. M.J. Schick, Nonionic Surfactants: Physical Chemistry, M. Dekker, New York, 1986.

86. P.A. Kralchevsky, J.C. Eriksson and S. Ljunggren, *Adv. Colloid Interface Sci.* 48 (1994) 19.

87. P.A. Kralchevsky, T.D. Gurkov and K. Nagayama, J. Colloid Interface Sci. 180 (1996) 619.

88. G.J.M. Koper, W.F.C. Sager, J. Smeets and D. Bedeaux, *J. Phys. Chem.*, 99 (1995) 13291.

89. O.D. Velev, T.D. Gurkov and R.P. Borwankar, *J. Colloid Interface Sci.* 159 (1993) 497.

90. O.D. Velev, T.D. Gurkov, I.B. Ivanov and R.P. Borwankar, *Phys. Rev. Lett.* 7 (1995) 264.

91. K.D. Danov, T.D. Gurkov, T.D. Dimitrova and D. Smith, J. Colloid Interface Sci. 188 (1997) 313.

92. J.N. Israelachvili and H. Wennerström, *J. Phys. Chem. 96* (1992) 520.

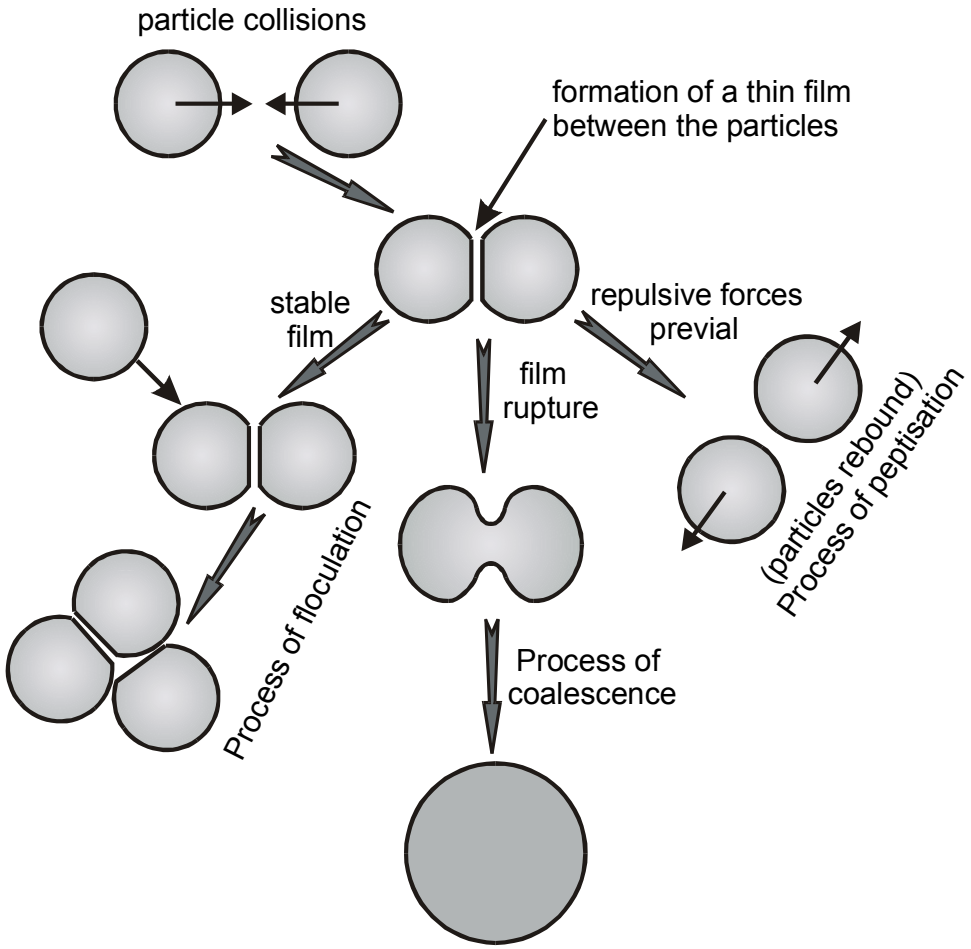

Fig. 1. Possible results of the collision of two emulsion droplets in connection with the droplet-droplet interaction.

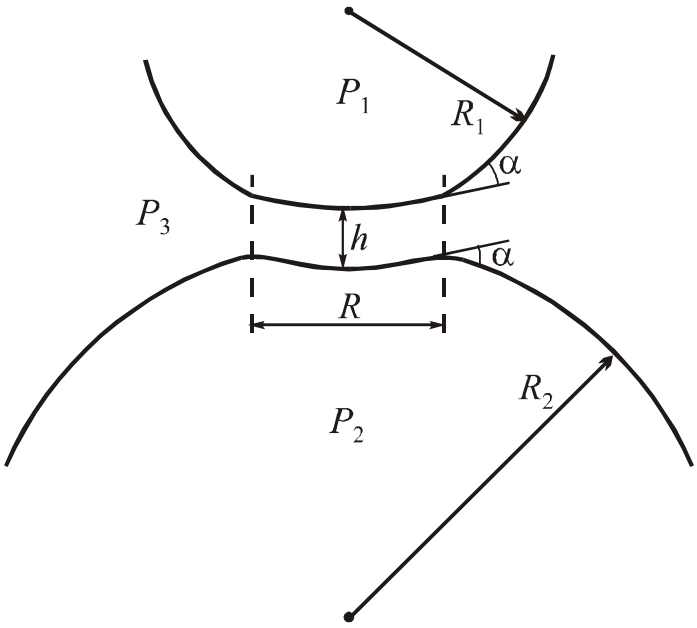

Fig. 2. Sketch of a film between two non-identical fluid particles of radii R_1 and R_2. The film thickness and radius are denoted by h and R.

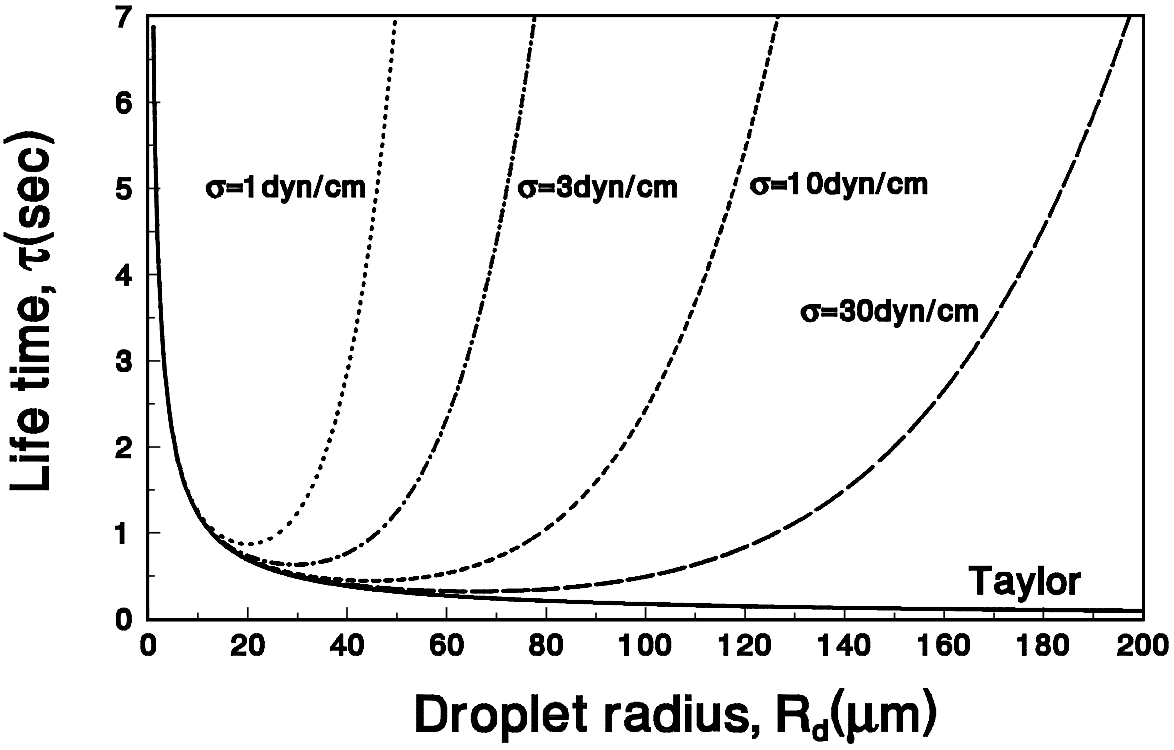

Fig. 3. Calculated life time, τ, of oil-in-water drops approaching from below an water-oil interface in Taylor regime (the solid line) and in Reynolds regime (the other lines) as a function of the droplet radius, R_d.

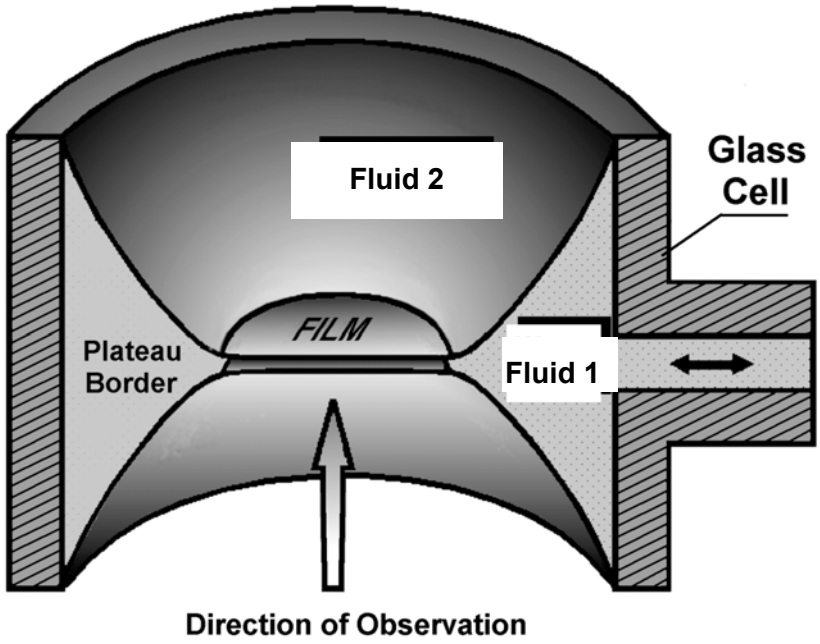

Fig. 4. Vertical section of the Scheludko cell [18]. The film (in the middle) is formed by ejection of Fluid 1 from an initially biconcave droplet through an orifice (on the right) in the cylindrical glass wall.

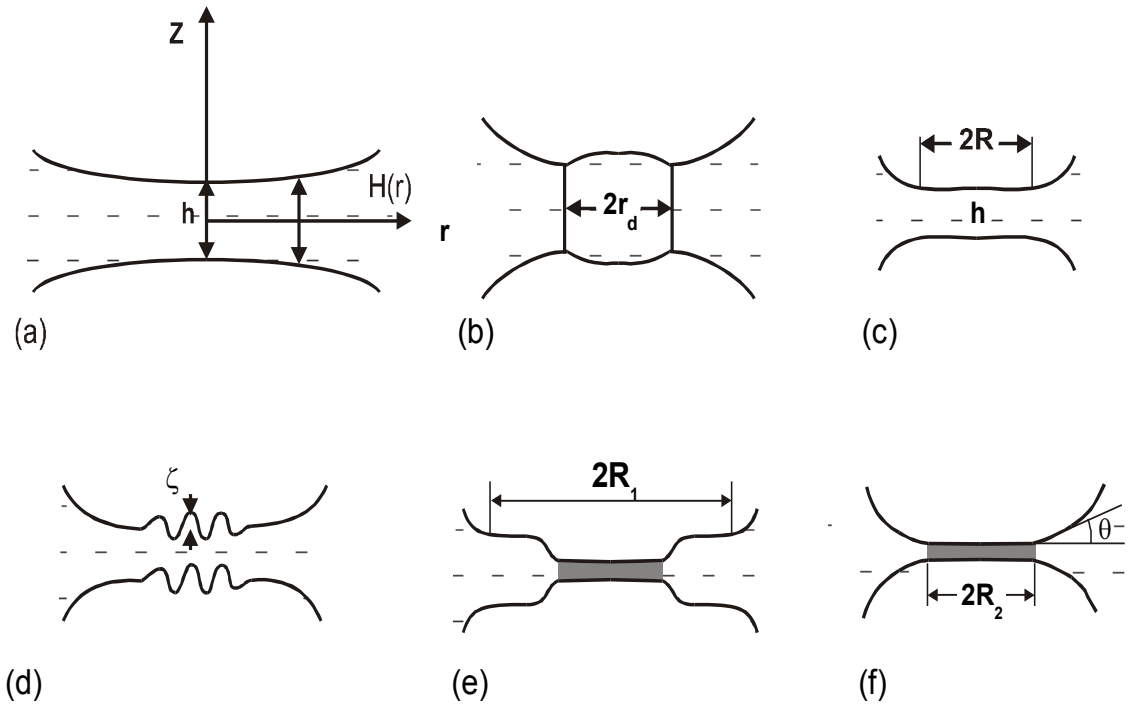

Fig. 5. Consecutive evolution stages of a thin liquid film between two drops or bubbles: (a) mutual approach of slightly deformed surfaces; (b) formation of a "dimple" in the center of the film; (c) the dimple disappears and an almost plane-parallel film forms; (d) due to thermal corrugations or outer perturbations the film either ruptures or transforms into a thinner Newton black film, which expands (e) until reaching the final equilibrium state (f).

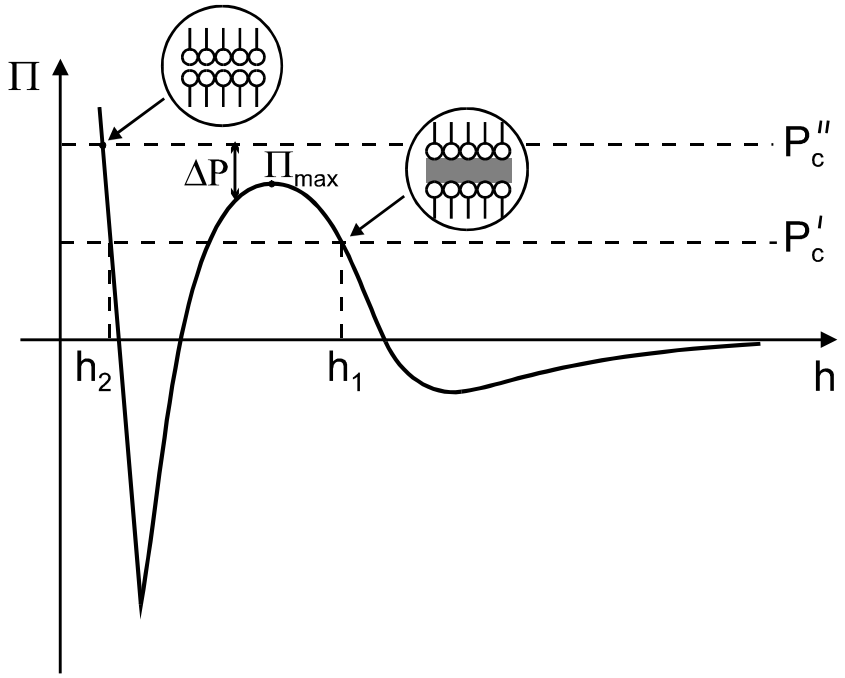

Fig. 6. Sketch of a disjoining pressure isotherm of DLVO type, Π vs. h. The intersection points of the Π(h)-isotherm with the line Π=P_c correspond to stable equilibrium films when $\partial\Pi/\partial h < 0$: h=h_1 - primary film, h=h_2 - secondary (Newton black) film.

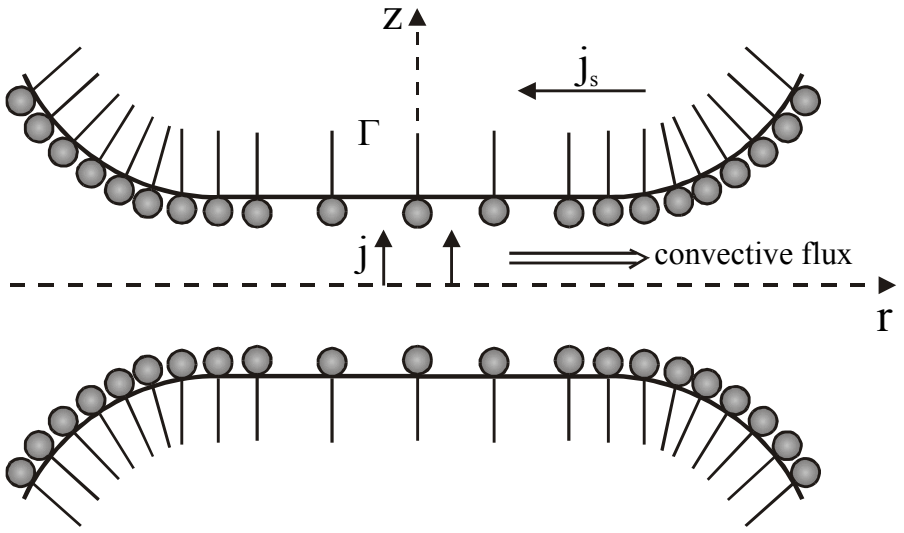

Fig. 7. Sketch of the zone of contact of two approaching fluid particles. The convective outflux of liquid drags the surfactant molecules along the two film surfaces; **j** and $\mathbf{j}_s$ denote the bulk and surface surfactant diffusion fluxes.

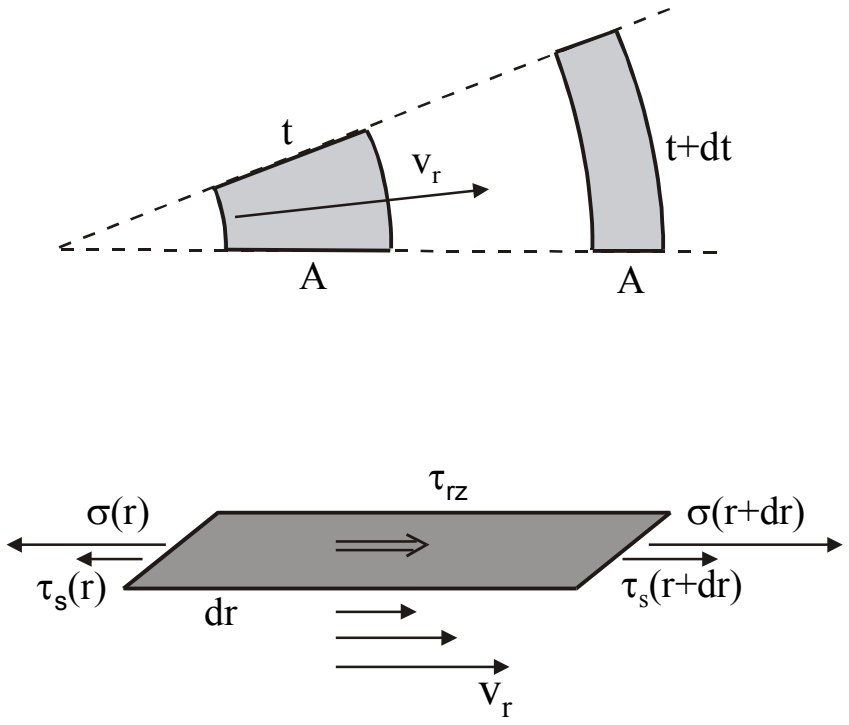

Fig. 8. Two consecutive positions of a surface element at time moments *t* and *t+dt*. The surface element experiences drag forces from the two adjacent bulk phases, as well as the action of the surface tension σ and surface viscous stress, τ_s, at its periphery.

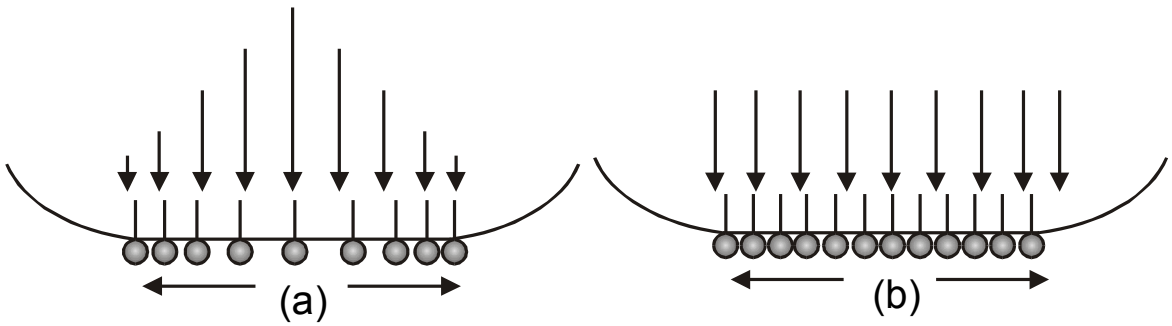

Fig. 9. Damping of convection driven surface tension gradients by influx of surfactant from the drop interior. (a) The mass transport is proportional to the perturbation. (b) Uniform surfactant distribution is quickly reached.

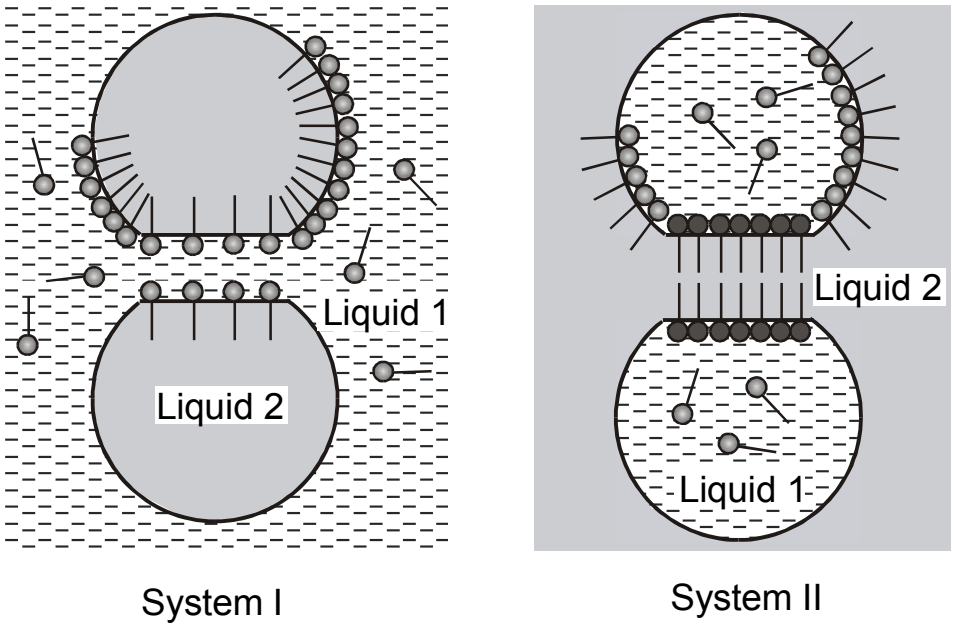

Fig. 10. Two complementary types of emulsion systems obtained by a mere exchange of the continuous with the disperse phase. The surfactant is assumed to be soluble into Liquid 1.

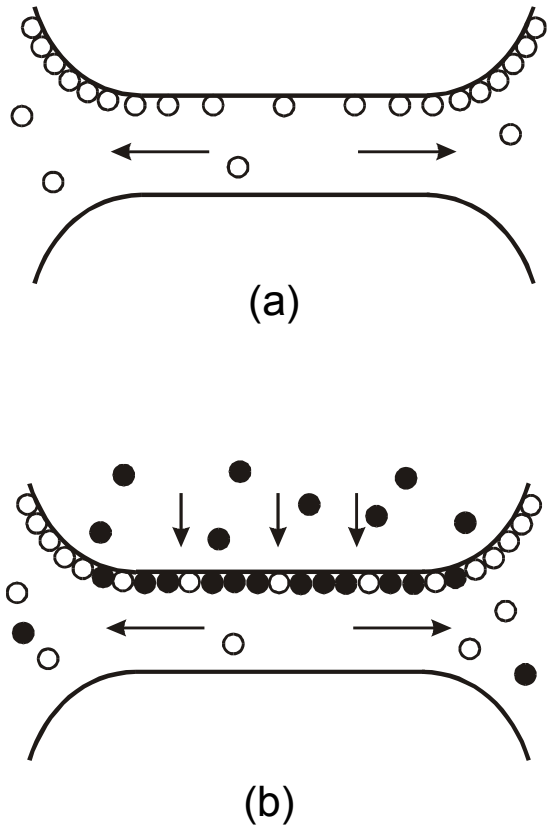

Fig. 11. (a) Non-uniform surface distribution of an emulsifier due to the drag from the draining film. (b) Damping of the surface tension gradient by a demulsifier (the black dots) added in the drop phase.

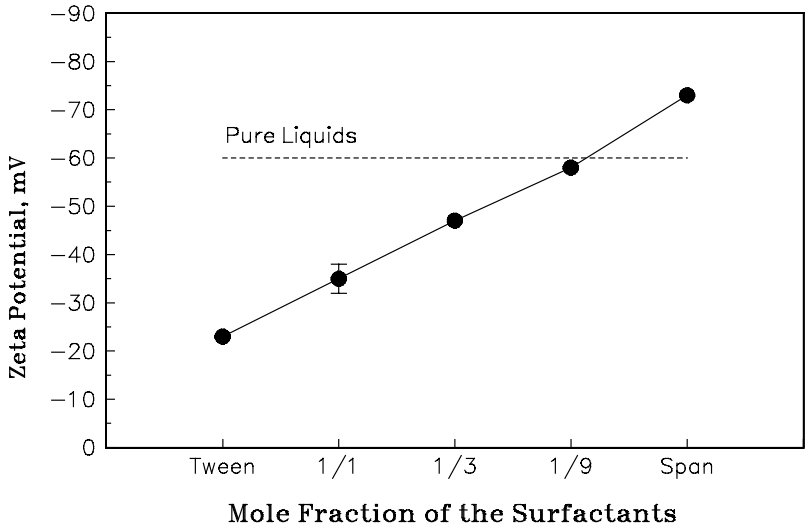

Fig. 12. Data for the ζ-potential of xylene droplets in aqueous solutions of the nonionic surfactants Tween 20 and Span plotted vs. the mole fraction of the surfactant mixture, after Ref. [54]. The total surfactant concentration is 0.1 mM and the concentration of the added NaCl is 1 mM.

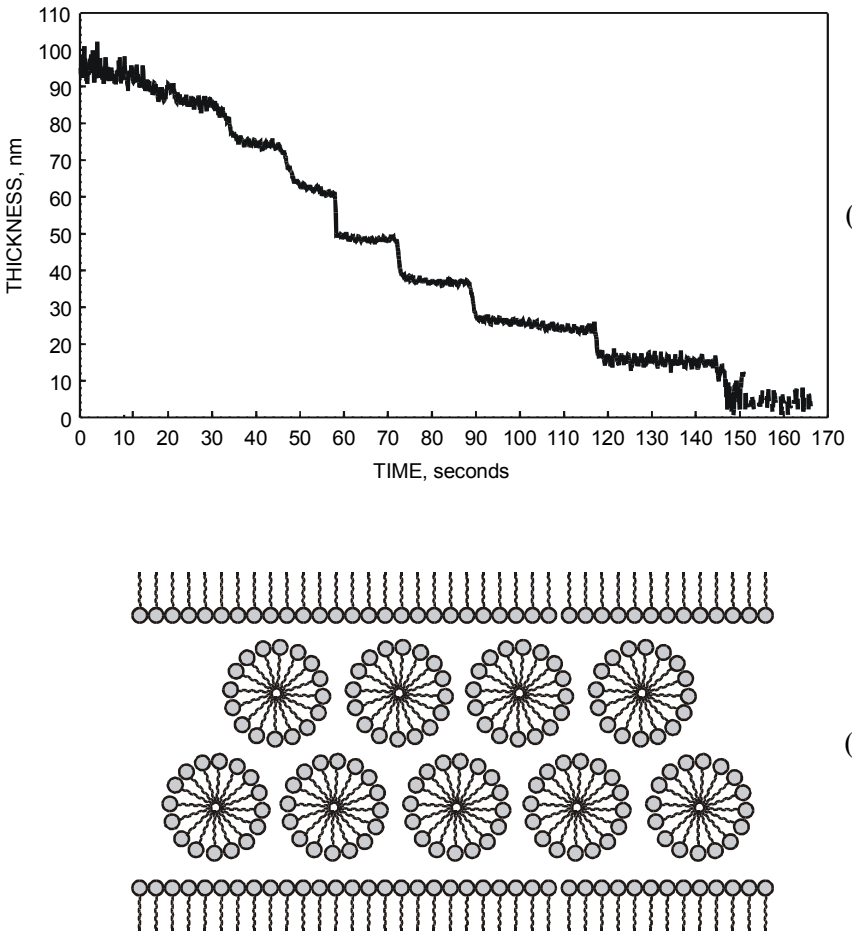

Fig. 13. (a) Experimental curve (from Ref. 77) showing the decrease of the thickness, *h*, of an emulsion film with time. The film is formed from 33.5 mM aqueous solution of sodium nonylphenol polyoxyethylene-25 sulfate with 0.1 M NaCl added. The "steps" of the curve represent metastable states corresponding to different number of micelle layers inside the film. (b) Sketch of a film containing two micelle layers.

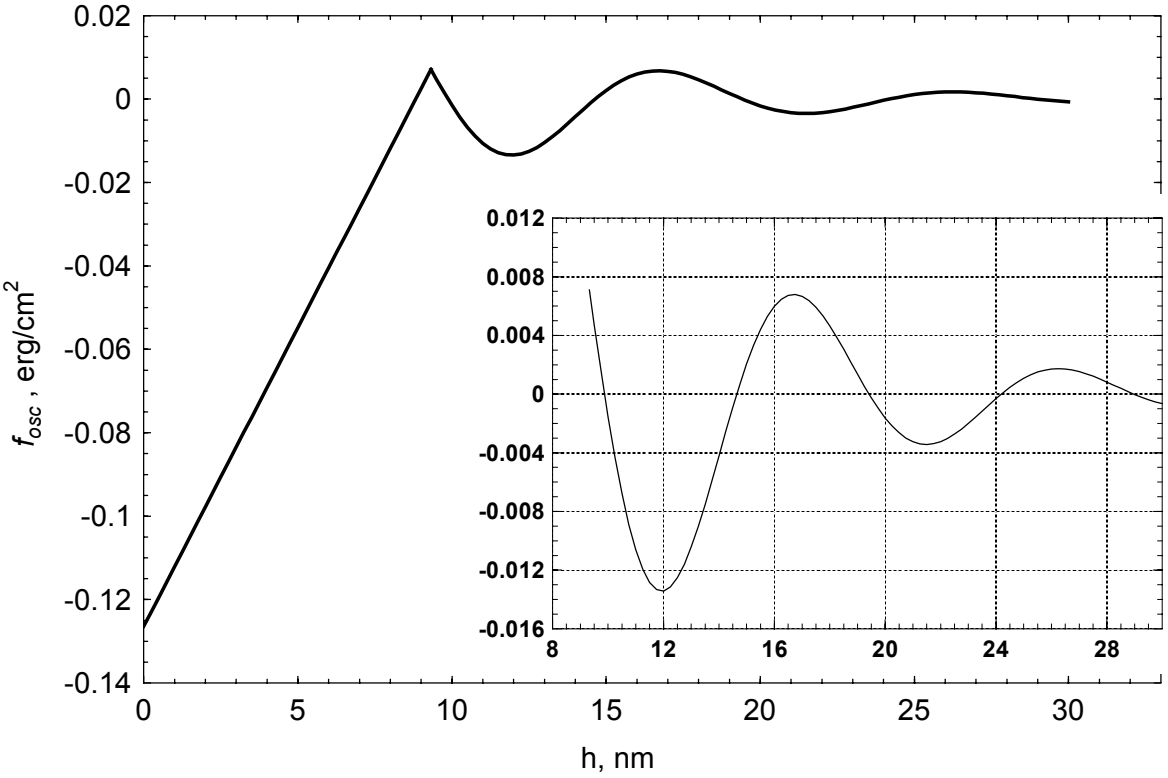

Fig. 14. Plot of the oscillatory free energy, f_{osc} , vs. the film thickness, h, calculated from Eqns (5.1)-(5.4) with the parameters values from Table 1 for φ=0.32. The inset shows the region 8 nm < h < 28 nm in an enlarged scale.

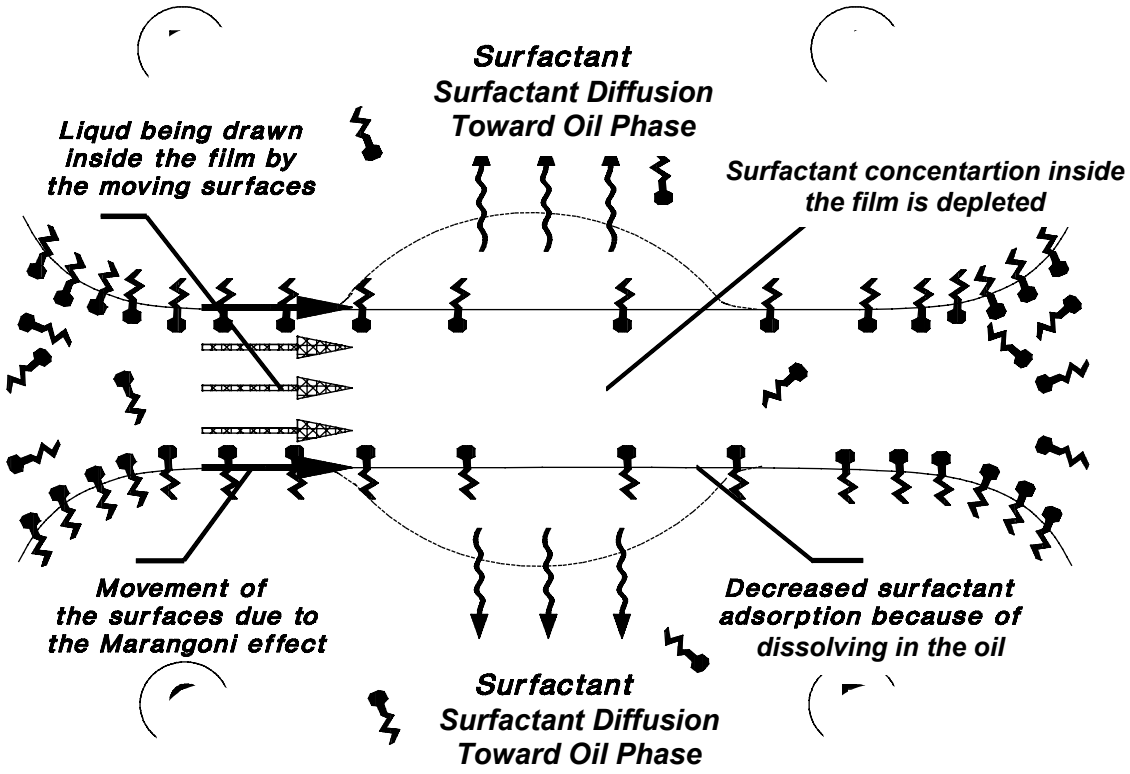

a

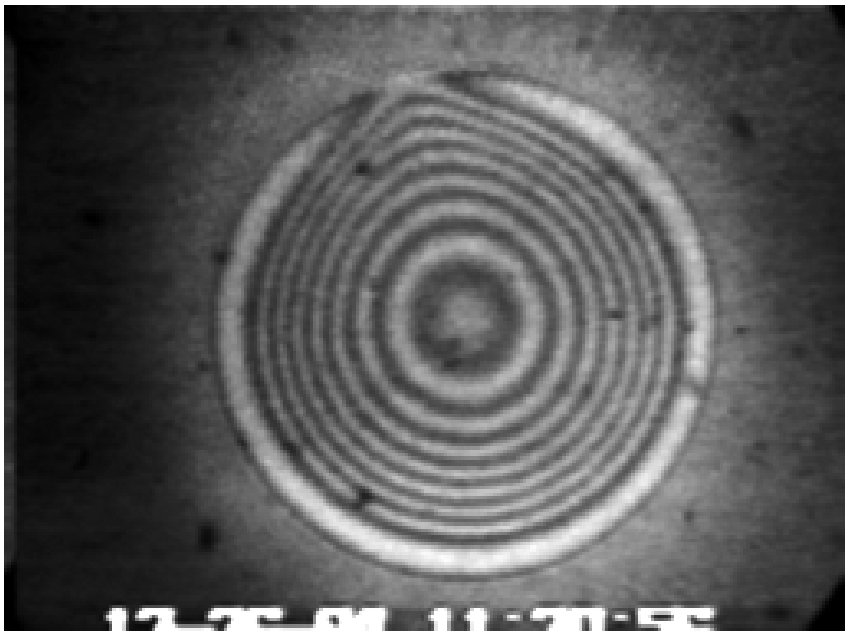

b

Fig. 15. Cyclic dimpling caused by the surfactant transfer from the aqueous film toward the two adjacent oil phases: (a) schematic presentation of the process; (b) photograph of the interference pattern in light reflected from a large dimple just before its flowing out.

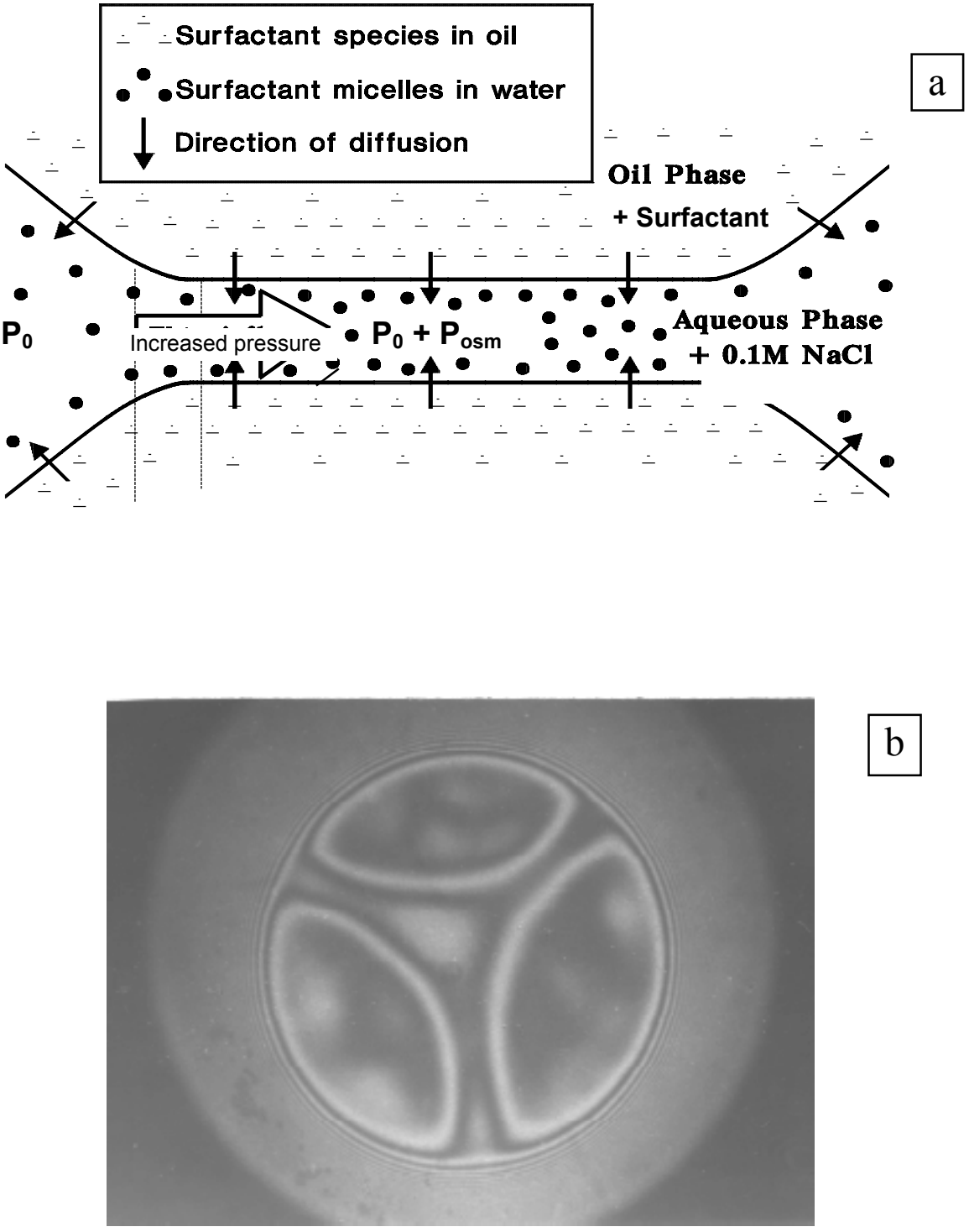

Fig. 16. Osmotic swelling of an aqueous film between two oil droplets: (a) The surfactant dissolved in the oil is transferred toward the film where micelles are formed; their osmotic effect increases the local pressure in the film. (b) Photograph of a typical pattern from a circular film with channels.